Research Article

Hexadecyltrimethyl Ammonium (HDTMA) and Trimethylphenyl Ammonium (TMPA) Cations intercalation of Nigerian Bentonite Clay for Multi-component Adsorption of Benzene, Toluene, Ethylbenzene and Xylene (BTEX) from Aqueous Solution: Equilibrium and Kinetic Studies

Kelechi E Onwuka*, Jude C Igwe, Chris U Aghalibe, Anthony I Obike

Department of Pure and Industrial Chemistry, Abia State University Uturu, P.M.B. 2000, Nigeria

***Corresponding Author:** Kelechi E Onwuka, Department of Pure and Industrial Chemistry, Abia State University Uturu, P.M.B. 2000, Nigeria; E-mail: onwukake@gmail.com

Received: 12 August 2020; **Accepted:** 21 August 2020; **Published**: 24 August 2020

Citation: Kelechi E Onwuka, Jude C Igwe, Chris U Aghalibe, Anthony I Obike. Hexadecyltrimethyl Ammonium (HDTMA) and Trimethylphenyl Ammonium (TMPA) Cations intercalation of Nigerian Bentonite Clay for Multi-component Adsorption of Benzene, Toluene, Ethylbenzene and Xylene (BTEX) From Aqueous Solution: Equilibrium and Kinetic Studies. Journal of Analytical Techniques and Research 2 (2020): 70-95.

Abstract

Presence of BTEX compounds in water is a global concern. The effectiveness of HDTMA and TMPA cations intercalated Bentonite, corresponding to 100% of CEC in the removal of Benzene, Toluene, Ethylbenzene and Xylene (BTEX) in aqueous solution was assessed. Batch experiments were conducted to determine the influences of contact time and adsorbate concentration on the adsorption efficiency. FTIR spectroscopy, SEM and XRD were used to determine the adsorbent properties. Results showed that surfactant modification of the adsorbent led to structural changes and fractional attainment to equilibrium showed that equilibrium was reached after 120mins. The sorption of BTEX by Bt-HDTMA and Bt-TMPA were in the order of B<T<E<X. The experimental data were fitted by many kinetic and isotherm models. The results also showed that pseudo-second-order kinetic model with highest R^2 values ranging from 0.883-0.997 for BTEX gave the

best fit to the experimental data compared to other available kinetic models. Freundlich isotherm model with highest R^2 values ranging from 0.979-0.993 for BTEX and n values from 0.55-1.55, fitted to the experimental data better than other isotherm models, confirming Freundlich isotherm as best fit to the sorption process and high efficiency of organoclays for BTEX removal.

Keywords: Hexadecyltrimethyl ammonium; Trimethylphenyl ammonium; Benzene, Toluene, Ethylbenzene and Xylene (BTEX); Isotherm; Bentonite

1. Introduction

Water is a vital resource for life but is increasingly being polluted by anthropogenic activities including oil spillage, urbanization, population growth, poor land use, and agricultural activities that have led to increased degradation of surface and ground water quality. The world faces serious problem of water scarcity for various purpose including household needs. This depends on economic growth, development climate change, season and human activity [1]. Owing to antropogenic activities, the vast amount of contamination discharge to the environment from various sources causing detrimental impact on the environment is a growing concern [1,2]. Water pollution consists of duel effects such as: on the environment and living organisms. In the aquatic systems the pollution affects the productivity, diminution and elimination of environmentally sensitive organisms. In the world, nearly 14,000 people died every day due to water pollution [1]. Various pollutants in water affect the water bodies by changing the properties, like algal blooming, pH changes, turbidity, TDS, conductivity, salinity, odor, sulphate content and carbon dioxide content [3]. Of all these anthropogenic activities mentioned above, hydrocarbon pollution from oil spillage and gas flaring remains a serious global concern with great priority in oil producing regions of the world [4], since larger hydrocarbon molecules like polycyclic and monocyclic hydrocarbons, are discharged into the environment. Most oil spills occur due to underground water well blowouts, tanker accidents, storage tank failures, production platform blowouts, intensified petroleum exploration on the continental shelf, transfer operations between ships and shores, economic sabotage and youth restiveness like the Niger Delta militias in South-South, Nigeria [5].

Hydrocarbons and volatile organic compounds (VOCs) play a crucial role among the substances determining water and soil pollution [6]. European Union regulations defines VOCs as the organic compounds which possess initial boiling point below or equal to 250°C at a standard atmospheric pressure of 101.3 kPa [7]. Generally, most VOCs are toxic or odorous and regarded as the main contributor of photochemical smog, ozone depletion and global warming. Chemical, pharmaceutical, petrochemical, adhesives production and wastewater treatment plants are the main sources of VOCs [6]. The petroleum hydrocarbon compounds are a group of organic constituents, which are components of gasoline and aviation fuels and are widely used in industrial syntheses. Crude oil, and in particular gasoline fraction is a main source of monoaromatic hydrocarbons, such as benzene, toluene, ethylbenzene and xylene (BTEX) [6,8]. These compounds are utilized as industrial solvents, serving as precursors for the production of many

pharmaceuticals, agrochemicals, polymers, explosives, paints, cosmetics etc [9,10]. Recent reports have shown high concentrations of BTEX compounds in soil, water, air [1,6,10-17] and even blood samples [18]. BTEX are frequently introduced into groundwater, soil and sediment via accidental spills and leakage from storage tanks and associated piping, improper waste disposal practice and leaching landfills as well as industrial effluent discharges [6,19-21]. In addition, studies such as Grady and Casey [22], Schmidt *et al*. [23], Mitra and Roy [24], and Reddy *et al*. [25] have reported the presence of BTEX compounds in drinking water, indicating extensive health risks that may not obvious. BTEX are known carcinogenic [18] and possess a negative health impact on human beings, other living organisms and the environment at large.

It is crystal clear that BTEX compounds are harmful to human health; long-term exposure may lead to respiratory and cardiovascular illnesses and also affects the function and development of the immune, metabolic and reproductive systems [10,24,26-28]. Recently, Ran *et al.,* [29] reported that short-term elevations in ambient BTEX concentrations may trigger failure of the respiratory system. Frequent exposure to BTEX compounds can cause neurological impairment while exposure to benzene can contribute to carcinogenicity, haematological effects including aplastic anaemia and acute myelogenous leukaemia [30,31]. Ethylbenzene and xylene could cause acute eye and skin irritation [26,29]. The health risk assessment (HRA) of BTEX (carcinogenic and non-carcinogenic) suggested by the United States Environmental Protection Agency (USEPA) is usually applied when estimating the nature and likelihood of adverse health impacts of each monitored BTEX compounds [10,27,32-34]. In addition to its adverse health implication, BTEX are also precursors to other air pollutants such as tropospheric ozone, polycyclic aromatic hydrocarbons, particulate matter, and ultrafine particles [10,26,35,36]. The exposure of BTEX can trigger acute and chronic effects to human health as indicated by many previous studies [10,26,37,38]. As a result, it is imperative that the remediation of these compounds in water is prioritized in future water treatment systems.

Numerous methods have been reported for BTEX removal from aqueous solutions [8,39,40]. Chemical oxidation, biological treatment, air stripping, and adsorption have been successfully carried out for the removal of BTEX from aqueous solutions [40]. Adsorption process is one of the prominent methods for the removal of these pollutants from the aqueous mediums because it is possible to recover the adsorbent and adsorbate [41]. Many adsorbents including activated carbon [42], carbon nanotube [43], nanoparticle electro-catalytic system [1], zeolite [15,16], macroreticular resins [12,41], diatomite [44], and organoclay [8,45-47] have been used for adsorption of BTEX from aqueous solutions. Activated carbon is widely and commonly used as an adsorbent for this purpose [45]; however, it is expensive and the regeneration cost is high [42]. Clay, owing to its high surface area, low cost, being eco-friendly, and nontoxicity, has a good efficacy in the adsorption of various pollutants in aqueous solutions [48]. Raw clay, due to the hydration of inorganic cations in its active sites, has a hydrophilic property. Therefore, it is not effective for the removal of nonpolar nonionic organic compounds such as BTEX. Hence, the modification of clay by a

surfactant, especially the cationic type, transforms it from the hydrophilic nature to the organophilic one [49], making it more suitable for sorption of BTEX compounds.

Many studies have been conducted by other researchers for the removal of BTEX with clay modified by cationic surfactants [8,45-47]. Organoclays, essentially 2:1 clays, have been widely used for the removal of BTEX compounds from aqueous solutions [8,40,46,50,51]. However, modification of bentonite clay with Trimethylphenyl ammonium chloride (TMPA-Cl) and Hexadecyltrimethyl ammonium bromide (HDTMA-Br) as cationic surfactants have not been poorly investigated. In this study, bentonite, in its natural and modified states was used as adsorbents for multi-component adsorption of benzene, toluene, ethylbenzene and xylene (BTEX) from aqueous solution, via batch adsorption experiment. Intra-particle diffusivity and effect of various conditions such as contact time and initial adsorbate concentration were investigated.

2. Materials and Methods

2.1 Preparation and Pre-Treatment of Adsorbent

The bentonite (Bt) clays exploited in this research was collected from Mansid Nigeria Limited, Port Harcourt Rivers State, Nigeria. In order to purify the clays, the method of Nourmoradi *et al.* [8] was adopted. 30g each of raw bentonite (Bt) was dissolved in 1L of distilled water and mixed with a magnetic stirrer (6000 rpm for 24h) at room temperature (25^0C). The Bt impurities such as iron oxide and silica, because of higher density were precipitated in the tube using a centrifuge rotating at 6000 rpm for 15 mins [53]. The impurities were removed and highly pure Bt dried at 110^0C for 24h, ground and sieved to a size of less than 125µm. The cation exchange capacity of Bt after purification was determined and compared with that of the raw Bentonite (before purification).

The pure Bt was pre-modified by adopting the methods of Baskaralingam [53]. High-purity Bt was mixed with sufficient amount of 1M NaCl using a mechanical stirrer (6000 rpm for 24h) at room temperature of 25^0C. The Na-Bt were then separated and washed four times with distilled water to remove any trace of chlorides, which was confirmed by the addition of 1M $AgNO_3$, resulting to the absence of a white or an off-white precipitate.

2.2 Organoclay preparation

2.2.1 Preparation of Surfactant Modified Bentonite Using HDTMA-Br and TMPA -Cl

HDTMA and TMPA organoclays were separately prepared according to the method of Banik *et al.*, [54], with little modification. 5g each of sodium exchanged bentonite (Na-Bt) were seperately dispersed in 400 mL of distilled water under continuous stirring for 4 h. The amount of HDTMA-Br and TMPA-Cl added respectively to each mixture were calculated with the CEC value (110 meq/100 g clay) of bentonite. Desired amount of each surfactant (HDTMA-Br and TMPA-Cl) were separately added to 200 mL of distilled water each in a separate container slowly. The reaction mixtures were stirred for 10 hours at 80ºC. The resulting products were separated individually by filtration and washed with distilled water for 3 times. Then the products were washed with ethanol. Synthesized organoclays (Bt-HDTMA and Bt-TMPA) were dried in an oven at

80ºC for 48 hours and grind into powder, stored in desiccators for characterization and further use.

2.3 Preparation of BTEX solution

Benzene (≥98%), toluene (98.5%), ethylbenzene (≥99%), and xylene (98.5%) were purchased from Sigma-Aldrich Chemical Company, Switzerland. The BTEX standard solution (400 mg/L BTEX = 100 mg/L benzene + 100 mg/L toluene + 100 mg/L ethylbenzene + 100 mg/L xylene) was prepared in distilled water and kept at 4^0C. The stock solutions were further diluted to prepare various working standard concentrations.

2.4 Adsorbent characterization and batch adsorption Studies

The surface areas of the Bt, Bt-HDTMA and Bt-TMPA were determined by Sear's procedure as follows: 0.5 g each of Bentonite (Bt); HDTMA modified bentonite (Bt-HDTMA) and TMPA modified bentonite (Mt-TMPA) were mixed with 50 ml of 0.1 M HCl solution on a magnetic stirrer and 10.0 g of sodium chloride salt was added to each mixture. The mixture was then titrated with standard 0.1 M NaOH solution in a water bath at 298±0.5 K from pH 4.0 to 9.0. The surface areas were measured by the following equation:

$$S = 32V - 25 \qquad (1)$$

where S (m^2/g) is the surface area of the adsorbent and V (ml) is the volume of NaOH solution required to increase the solution pH from 4.0 to 9.0 [55].

Possible variations in the functional groups of the adsorbents were assessed by Buck scientific M530 USA FTIR. This instrument was equipped with a detector of deuterated triglycine sulphate and beam splitter of potassium bromide. The software of the Gram A1 was used to obtain the spectra and to manipulate them. An approximately 1.0 g each of Bt, Bt-HDTMA and Bt-TMPA were properly placed on the salt pellet. During measurement, FTIR spectra was obtained at frequency regions of 4,000-600 cm^{-1} and coded at 32 scans and at 4 cm^{-1} resolution. FTIR spectra were displayed as transmitter values.

The compositions of the adsorbents were also identified by X-ray defractometer (Bruker, D8ADVANCE Germany). 20 mg each, of Bt, Bt-HDTMA and Bt-TMPA were ultrasonically dispersed in I mL of 95% ethanol and dried as oriented aggregates on 2.5 cm-diam. Circular glass slides, separately. 20 mg of the raw and modified clays were dispersed in 1 mL of water and dried on glass slides. Basal x-ray diffraction spacings were then recorded using Ni-filtered Cu K$\alpha\alpha$ radiation (1.5406 Å), x-ray diffractometer with a graphite monochromator, a solid state detector, and an autosampler. Digital intensity and $^o2\theta$ values from 2 to 20 $^o2\theta$ x-ray scans were recorded on disk and were later used with a graphics program to print x-ray diffraction patterns. Because organo-clays often yield low angle peaks that correspond to very large (>18 Å) basal spacings. The diffractomerer was aligned using a cholesterol standard [56] to ensure accuracy of the x-ray data at low $^o2\theta$ values.

Surface topographical information was obtained by a surface morphological study using Scanning Electron Microscope (Seron, AIS-2100, Republic of Korea). Bt, Bt-HDTMA and Bt-TMPA were separately placed on a sample stub with the aid of a graphite conductive adhesive paste before being firmly loaded

on a cylindrical rod which serves as the sample holder. The rod was thereafter placed in the analysis chamber of the SEM which remains under vacuum all through the analysis. When excited primary beam of electrons from the light source strikes a sample, various secondary electrons from the sample surfaces were emitted which are characteristic of each of the samples. Various secondary electron detectors attract the scattered electrons, and the signals were used to form images of the specimen.

Batch adsorption tests were carried out to examine the adsorption efficiency of the raw and surfactant modified clays (Bt, Bt-HDTMA and Bt-TMPA). All adsorption experiments were carried out at room temperature (25^0C) with 100 mL of BTEX solution into a 200 mL conical flask (with air tight cape) and shaken at 250 rpm for 24 h. After this, the suspensions were centrifuged (6000 rpm for 15 min) and the clear supernatant was then measured for BTEX by Gas chromatography (Agilent GC, 6890N), equipped with mass spectrometer detector.

The GC-MS method for determination of BTEX was optimized as follows:
(i) Sampling method: head space;
(ii) Injected sample volume: 250 μL;
(iii) Carrier gas: helium (purity 99.995%) with flow rate of 1.11 mL/min;
(iv) GC column *characteristic*: Agilent HP-5 MS UI 30m x 0.250m,-60 to 325/350^{0}C;
(v) Oven temperature: 200^{0}C.

Blank samples (BTEX solution without the adsorbent) were also utilized to determine the value of BTEX volatilization. The BTEX loss due to the volatilization was estimated in percentage. The experimental data were corrected to account for BTEX loss occasioned by volatilization. The adsorption capacities of Bt, Bt-HDTMA, and Bt-TMPA for BTEX uptake were determined using:

$$q_e = \frac{(C_o - C_e)V}{m} \qquad (2)$$

Where q_e (mg/g) is the adsorption capacity of the adsorbent, C_o (mg/L) is the initial concentration of the adsorbate, C_e (mg/L) is the equilibrium concentration of the adsorbate in the solution, m (g) is the mass of the adsorbent, and V (L) is the volume of the solution.

The effect of contact time on the adsorption of BTEX by Bt, Bt-HDTMA and Bt-TMPA was carried out, using 100 mL of a solution containing 0.5 g adsorbent and 50 mg/L BTEX solution (Benzene 10 mg/l, Toluene 10 mg/l, Ethylbenzene 10 mg/l and Xylene 20 mg/l) at various contact times of 10, 20, 40, 60, 100 and 120 mins.

In many industrial wastewaters the concentration of BTEX varies between 20 to 200 mg/L [43]. Hence, the effect of initial BTEX concentrations of 50, 100, 125, 150, and 200 mg/L on the adsorption efficiency was examined at optimum contact time and pH at at room temperature (25^0C).

3. Results and Discussion

3.1 Adsorbent Characterization

Table 1, show the values for surface areas for bentonite (Bt), HDTMA modified bentonite (Bt-HDTMA) and TMPA modified bentonite (Bt-TMPA). The modification of the adsorbents by Haxadecyltrimethylanonium bromide and

Trimethylphenylamonium chloride led to increment in surface area from 327m^2/g for Bt to 512.6m^2/g and 384.6m^2/g for Bt-HDTMA and Bt-TMPA respectively, suggesting the occurrence of micropores in the interlayer between organic cations. From the values obtained for CEC of bentonite (Bt), HDTMA modified bentonite (Bt-HDTMA) and TMPA modified bentonite (Bt-TMPA) in Table 1, an increase in cation exchange capacity (CEC) from 30.94 meq/100g for Bt to 55.01meq/100g and 47.57meq/100g for Bt-HDTMA and Bt-TMPA respectively was observed, corresponding to the values obtained by Nourmoradi *et al*. [8]. Due to the favorable interlayer microenvironment created by the long chain alkyl ammonium ions for the partitioning of organic molecules, the size of the alkyl chain and the charge density of the clay layer are responsible for the arrangement of the intercalated cations corresponding to increase in the clay cation exchange capacity.

Table. 1. Chemical composition of raw bentonite used in this study

Chemical composition (%)	Bentonite
SiO_2	48.87
Al_2O_3	14.98
Fe_2O_3	5.05
Na_2O	2.53
MgO	1.99
P_2O_5	1.1
K_2O	1.76
CaO	1.81
TiO_2	0.84
MnO	
H_2O	

	Adsorbents		
Others	Bt	Bt-HDTMA	Bt-TMPA
CEC (Meq/100g)	30.94	55.01	47.57
Surface Area (m^2/g)	327	512.6	384.6

The SEM images of bentonite (Bt), TMPA modified bentonite (Bt-TMPA) and HDTMA modified bentonite (Bt-HDTMA) are presented in Figures 1a, 1b and 1c respectively. The surface structure of the adsorbent is changed by the modification with HDTMA and TMPA. It is evident that the surface texture of bentonite (Bt) is rough with irregular shapes. However, the surface morphologies of HDTMA modified bentonite (Bt-HDTMA) and TMPA modified bentonite (Bt-TMPA) are smoother than unmodified bentonite (Bt). This is due to the fact that the porous surface of bentonite is occupied with surfactant. Similar results have been reported by Aivalioti *et al*. [44] and Nourmoradi *et al*. [8].

XRD patterns of bentonite (Bt), HDTMA modified bentonite (Bt-HDTMA) and TMPA modified bentonite (Bt-TMPA) samples are shown in Figure 1d. The XRD basal spacing (d_{001}) of Bt, Bt-HDTMA and Bt-TMPA were found to be 10.006Å, 14.172Å

and 13.285Å respectively. There was also a noticeable increase in the reflection intensity from 5.34% for Bt to 100 % for both Bt-HDTMA and Bt-TMPA respectively indicating structural changes in the bentonite clay, occasioned my surfactant modification. The interlamellar expansion in the modified adsorbent is attributed to the penetration of haxadecyltrimethyl ammonium cation and trimethylphenyl ammonium cation into the layers of Bt. The values of basal spacing obtained are in agreement with that reported by Taleb [57]. The cation exchange reactions have been frequently used as an effective method to replace inorganic ions with organic cationic surfactant molecules which intercalate into the clay gallery, resulting in expansion of the interlayer spacing thereby resulting to an increase in the basal spacing [58-61].

IR spectra peak for unmodified bentonite clay shows that the -OH bending band at 871cm^{-1} respectively were assigned to Al-OH. The shape and position of the -OH stretching band in the IR spectra of bentonite are are affected by the nature of the octahedral atoms to which the hydroxyl groups are domiciled [62,63]. The strong band located at 1059.7cm^{-1} for bentonite was consequent of Si-O stretching vibrations, indicating that Si-O-Al and Si-O-Si bending vibrations respectively were typical of the tetrahedral Si-O. Bands at 3365.3cm^{-1}, 1611.03cm^{-1} for bentonite are attributed to the OH stretching and bending vibrations of molecular water respectively. The quantity of adsorbed water in the clay is attributed to the deformation vibration of the H-O-H group (around 1631 cm^{-1}). Organo-modification of Bt with HDTMA and TMPA cations (Figures 1e.) increased the intensity at around 2901.29cm^{-1}, 2743.77cm^{-1} and 2939.7cm^{-1}, 2806.7cm^{-1} respectively in HDTMA modified bentonite (Bt-HDTMA) and TMPA modified bentonite (Bt-TMPA), corresponding to asymmetric and symmetric stretching of methylene (CH_2) bond [60,63]. Also a bending vibration of the methylene groups can be observed at bands of 1475 cm^{-1} for bentonite (Bt), confirming intercalation between cationic surfactants and clay layer [63,64]. Other bands in the 1149-600 cm^{-1} region are the Si-O stretching bands at around 1149 cm^{-1} (in-plane) and 914 cm^{-1} (out-of-plane), the Al-O+Si-O out-of-plane vibration at 607.59cm^{-1} for bentonite (Bt) respectively. IR spectra analysis justified the existence of a strong affinity between organic modifiers (HDTMABr and TMPACl) and bentonite when placed in its interlayer space and this consequently results to the formation of a new substance, which, because of the different structure relative to the clays and the monomers, will exhibit different characteristics [63,65,66].

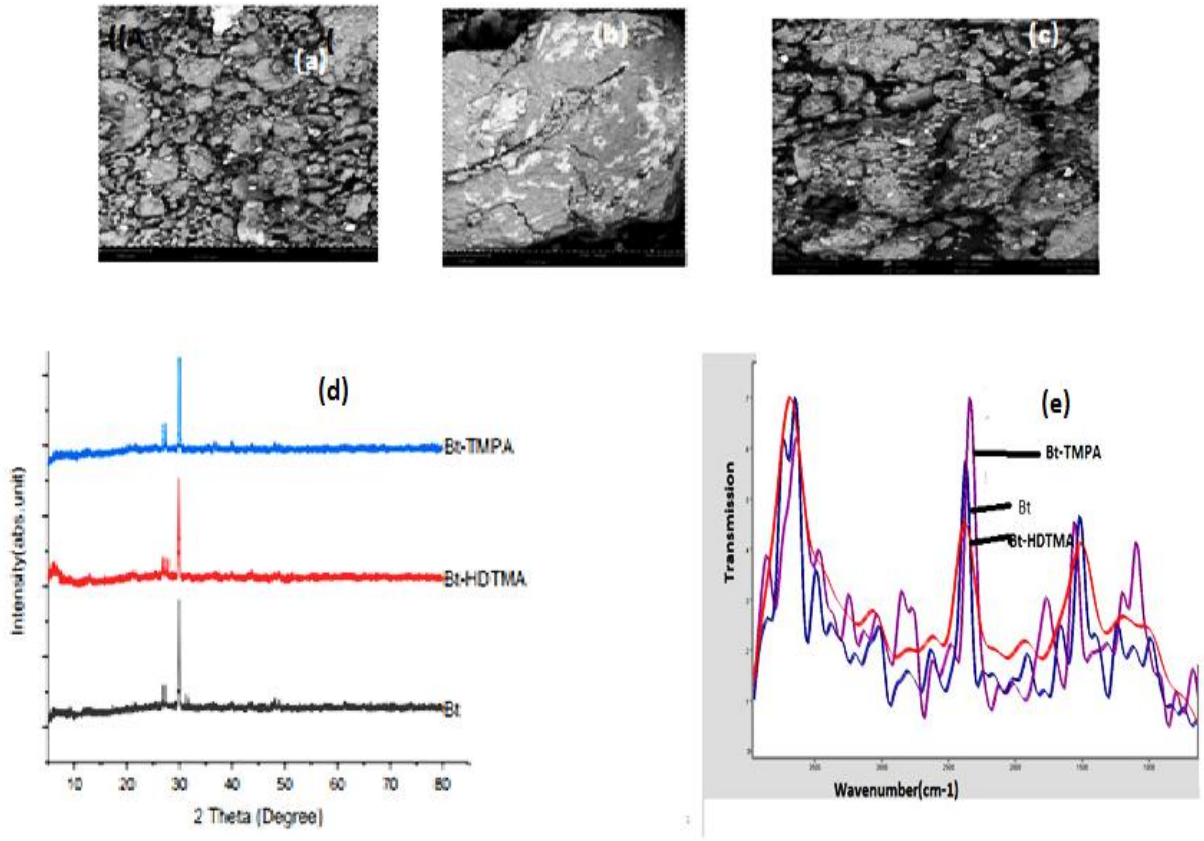

Figure 1: SEM Images of Bt (a), Bt-TMPA (b) and Bt-HDTMA (c); XRD patterns of Bt, Bt-HDTMA, Bt-TMPA (d) and FT-IR spectra of Bt, Bt-HDTMA, Bt-TMPA (e).

3.2 Effect of Contact Time

The efficiency of BTEX removal by bentonite (Bt), HDTMA modified bentonite (Bt-HDTMA) and TMPA modified bentonite (Bt-TMPA) are shown in Figures 2a, 2b and 2c respectively. It was noticed that increase in the contact time of the Bt, Bt-HDTMA and Bt-TMPA in the BTEX solution from 10-120 mins resulted in a dramatic increase in the amount of BTEX being adsorbed. The adsorption capacities of Bt, Bt-HDTMA and Bt-TMPA at the first 60 mins of the adsorption was found to be 0.092 mg/g, 0.090 mg/g, 0.13 mg/g, 0.473 mg/g, 1.442 mg/g, 1.49 mg/g, 1.542 mg/g, 3.672 mg/g, 1.434 mg/g, 1.676 mg/g, 1.74 mg/g, 3.556 mg/g for benzene, toluene, ethylbenzene, and xylene, respectively. The corresponding adsorption capacity at the equilibrium time was estimated to be 0.10 mg/g, 0.108 mg/g, 0.142 mg/g, 0.496 mg/g; 1.526 mg/g, 1.576 mg/g, 1.686 mg/g, 3.741 mg/g; 1.522 mg/g, 1.996 mg/g, 2.014 mg/g, 4.370 mg/g; thereby decreasing the concentration of the BTEX solution. The relatively high removal of BTEX is attributed to the availability of large number of vacant sites for adsorption of BTEX and at some point, reaches a constant value beyond which no more is removed from solution. At this point, the amount of the BTEX desorbing from

the adsorbent is in a state of dynamic equilibrium with the amount being absorbed by the adsorbent [63,67]. Equilibrium was attained at 120 mins in both Bt, Bt-HDTMA and Bt-TMPA. This can be explained by the fact that initially, the rate of BTEX uptake was higher because all sites on the adsorbent were vacant and BTEX concentration was high but decrease of adsorption sites declined the uptake rate. Similar results have been reported in previous studies [8,63,68]. The order of the sorption capacities of the modified adsorbents are B < T < E < X. This order may be attributed to water solubility [8,43], B (1790 mg/L) > T (530 mg/L) > E (152 mg/L) > X (150.5 mg/L) and the corresponding nature of hydrophobicity (based on log k_{ow}) calculated as B = 2.13, T = 2.69, E = 3.15, and X = 3.15 [44]. Many previous studies have confirmed that the sorption of BTEX from aqueous solutions with various adsorbents (Table 3.), follows a similar trend as above [8,40,42-44].

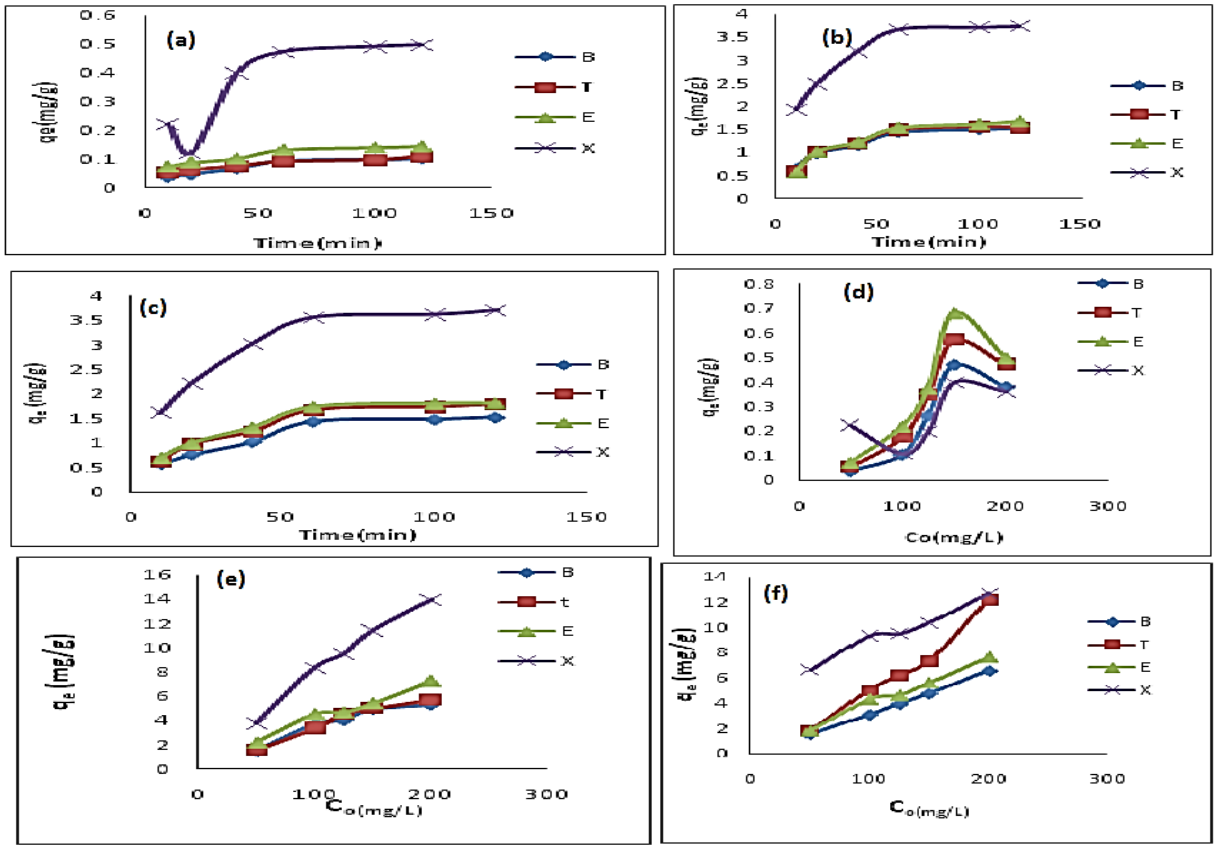

Figure 2: Effect of contact time on adsorption of BTEX using Bt (a), Bt-HDTMA (b), and Bt-TMPA (c), (BTEX solution = 50mg/L, initial pH= 7±0.5, contact time = 2hours, Bt =0.5g); Effect of BTEX concentration on adsorption by Bt (d), Bt-HDTMA (e), and Bt-TMPA (f), (Initial pH= 7± 0.5, contact time= 2 hours Bt conc = 5g/L)

BTEX adsorption by various adsorbents is presented in Table 2. As seen, the adsorption capacity of BTEX with the modified clays in this study is high, especially for Ethylbenzene and Xylene. The removal efficiency of BTEX by TMPA-clay and Adam-clay, is nearly equal with values obtained for Bt-HDTMA and Bt-TMPA. However the uptake efficiency for carbon nanotube (CNTNaOCl) and OMC-2NC were much higher than those of Bt-HDTMA and Bt-TMPA. Also, BTEX uptake efficiency by Bt-HDTMA and Bt-TMPA were higher than those of Angico sawdust (Su *et al*., 2010), peat (Su *et al*., 2010), mature compost (Bandura *et al*., 2017) and diatomite (Aivalioti et al., 2012). The effect of contact time on removing BTEX by raw Bt showed that the adsorption capacity of the raw adsorbents for these compounds were about 7 to 10 times less than that for Bt-HDTMA and Bt-TMPA. Therefore, 120 minutes was used as the optimum time for the other experiment.

3.3 Effect of Initial BTEX Concentration

Figures 2d, 2e and 2f displays the effects of initial BTEX concentrations between 50 and 200 mg/L on the sorption using bentonite (Bt), HDTMA modified bentonite (Bt-HDTMA) and TMPA modified bentonite (Bt-TMPA) at initial pH of 7 ± 0.5 for 120 minutes. From the results, the initial concentration of BTEX has important role on the adsorption capacity. As seen, the adsorption capacities of the sorbents were increased by increasing BTEX concentration in the solution. This may be attributed to increase in driving forces (van der Waal's force) affecting BTEX compounds and active adsorption sites of the adsorbent, which occurs at optimum concentrations [8,42].

Table 2. Comperison of BTEX removal from aqueous solution by adsorbents used in this study to thosse of other studies

Adsorbent	B(mg/g)	T(mg/g)	E(mg/g)	X(mg/g)	Conditins	References
TMPA-clay	1.13	8.65	3.18	4.24		[46]
Adam-clay	0.47	4.32	1.59	2.44		[46]
Diatomite	0.031	0.037	0.042	0.042-0.09	6hours 5mg/L	[40]
CNT(NaOCl)	200	220	250	270	C0=100 µg/l	[43]
Activated carbon	4.5	5	6	6.5	3hours 5mg/L	[40]
TTAB-Clay	3.98	5.15	6	6.98	24hours 150mg/L	[8]
HDTMA-Kao	9.202	0.697	0.147	0.042	30 min 0.01mg/L	[70]
Angico sawdust	0.00342	0.0041	0.00577	0.0107	C0=100 µg/l	[43]
Peat	0.00341	0.0047	0.00581	0.0119	C0=100 µg/l	[43]
Mature compost	1.12	1.59	2.16	3.5	C0=10 mg/l, T=20 °C, S/L=1/4 g/l	[69]
Modified diatomite	0.0468	0.0552	0.0849	0.276	C0=5 mg/l, S/L=50/1 g/l	[71]
OMC-2NC	12.7	32.9	37.7	58.7	C0=10 mg/l, T=25 °C, S/L=1/4 g/l	[72]
Bt-HDTMA	1.53	1.58	1.69	3.74	2 hours 50mg/L	This Study
Bt-TMPA	1.52	2	2.01	4.37	2 hours 50mg/L	This Study

3.4 Adsorption Kinetics

Adsorption kinetics is one of the most vital parameters for determining the adsorption mechanism and also to investigate the efficacy of adsorbent for the removal of pollutants [8]. In this study, three kinetic models; pseudo-first-order,

pseudo-second-order, and intra-particle diffusion models, were used to predict the sorption behavior of the data. The pseudo-first-order kinetic model known as the Lagergren equation [55] is defined as:

$$log(q_e - q_t) = log\ q_e - \left(\frac{k_1}{2.303}\right)t \qquad (3)$$

Where is the amount of BTEX adsorbed at equilibrium (mg/g), q_t amount of BTEX adsorbed at any given time t (mg/g), k is the rate constant for the pseudo-first-order model. A plot of ($q_e - q_t$) against t gives a linear slope (Figures 3a and 3b) from which the values of k_1 and q_e can be determined from the slope and intercept.

The pseudo-second-order model was also fitted to the sorption data using the following equation [73]:

$$\frac{1}{q_t} = \frac{1}{k_2 q_e^2} + \frac{t}{q_e} \qquad (4)$$

where q_e and q_t are the same as for the pseudo-first-order parameters. k_2 (g/mg^{-}h) is the rate constant of pseudo-second order. In Figures 3b and 3c, q_2 and q_e values were obtained from the intercept and slope of linear plot of t/q_t against t, respectively [8]. At initial stage of the adsorption process ($t \backsim 0$), the initial adsorption rate, h (g/mg $^{-}$h), is obtained from;

$$h = k_2 q_e^2 \qquad (5)$$

The intra-particle diffusion kinetic model is mathematically described by the following equation [8]:

$$q_t = k_{id} t^{1/2} + C \qquad (6)$$

where k_{id} (g/mg^{-}h) is the rate of the intraparticle diffusion kinetic model [43]. k_{id} and C are obtained from the slope and intercept of q_t versus $t^{1/2}$, respectively.

Figures 3c and 3d show plots of pseudo-second-order kinetic model for the adsorption of BTEX with Bt-HDTMA and Bt-TMPA. As can be seen from the correlation coefficient (R^2), the pseudo-second-order kinetic model gave the best fit to the experimental data, compared to other available kinetic models (Figures 3, a-f). Moreover, the $q_{e,calculated}$ (mg/g) achieved using the pseudo-second-order kinetic model is rationally similar to the $q_{e,experimental}$ (mg/g) obtained from the experimental data. On the other hand, the pseudo-first-order and intra-particle diffusion models, because of the significant variations between calculated q_e from the models and experimental q_e, do not suitably predict BTEX sorption by the adsorbent. Aivalioti *et al*. [44] and Nourmoradi *et al*. [8] reported that sorption of BTEX with raw and thermally modified diatomite, and raw and TTAB modified montmorillonite respectively were described well by the pseudo-second-order kinetic model [8,44]. The parameters for pseudo-second-order kinetic model are listed in Tables 3, for Bt-HDTMA and Bt-TMPA. As seen, the values of the rate constant for pseudo-second-order kinetic models, k_2 (g/mg.h), follow the order of B > T > E >X, while the initial adsorption rate constant values of this kinetic model, h (g/mg $^{-}$h), are shown to have the order of B < T < E < X.

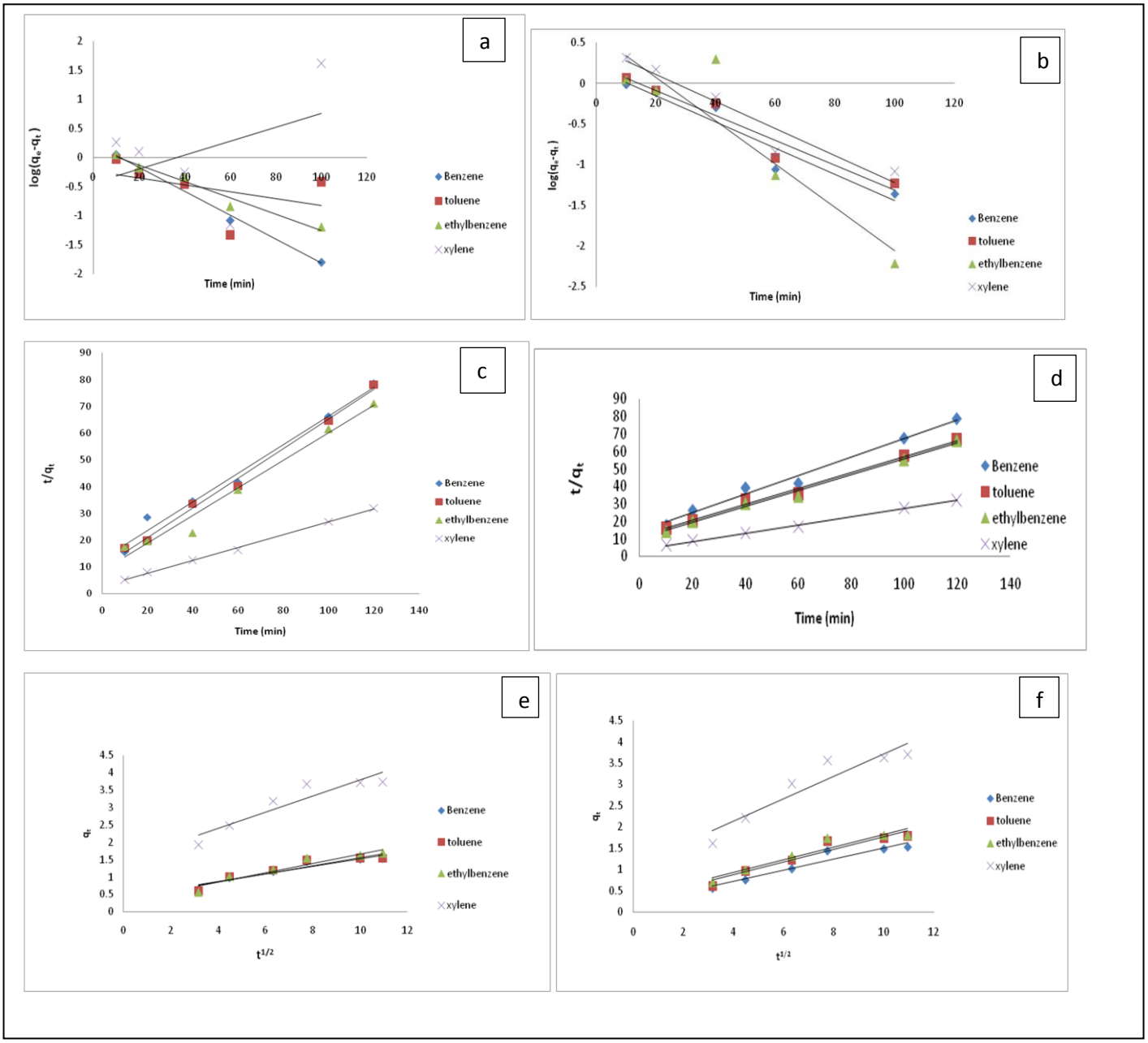

Figure 3: Kinetic models for adsorption of BTEX unto: Bt-HDTMA- Pseudo first order (a), Bt-TMPA-Pseudo first order (b), Bt-HDTMA-Pseudo second order (c), Bt-TMPA-Pseudo second order (d), Bt-HDTMA-Intra-particle diffusion (e), Bt-TMPA-Intra-particle diffusion (f).

The order of h values may be attributed to availability of more active vacant sites on the adsorbent at the beginning of the sorption process [8,74]. Hence, the lower hydrophilic compounds such as xylene and ethylbenzene have a higher tendency to the adsorbent, especially at the start of the adsorption process. But as the time elapsed, the order of k_2 value has an inv inverse relation with the order of h value. This may be attributed to the molecular weight of BTEX. Owing to lower molecular weight [8], benzene and then toluene can penetrate better onto the internal adsorption sites of the adsorbent compared to higher-molecular weight compounds such as ethylbenzene and xylene.

Table 3. Pseudo first order, second order and intraparticle diffusion parameters for the adsorption of BTEX by Bt-HDTMA and Bt-TMPA

	ADSORBENT	Bt-HDTMA				Bt-TMPA			
	ADSORBATE	Benzene	Toluene	Ethylbenzen	Xylene	Benzene	Toluene	Ethylbenzene	Xylene
Kinetic Models	**Parameters**								
Pseudo first Order									
	k_1	-0.02	-0.06	-0.014	0.011	-0.016	-0.015	-0.026	-0.016
	q_e	1.267	0.795	1.16	0.65	1.188	1.249	1.849	1.564
	R^2	0.982	0.184	0.965	0.179	0.925	0.94	0.833	0.928
Pseudo second Order									
	k_2	0.043	0.034	0.031	0.021	0.092	0.018	0.015	0.014
	$q_{e\ cal}$	1.862	1.802	1.937	4.149	1.88	2.198	2.198	4.24
	h	0.149	0.11	0.116	0.362	0.071	0.087	0.093	0.25
	$q_{e\ exp}$	1.526	1.576	0.1686	3.742	1.522	1.796	1.814	3.7
	R^2	0.984	0.994	0.977	0.997	0.922	0.92	0.91	0.883
Intra-particle diffusion									
	K_{id}	0.109	0.115	0.134	0.232	0.128	0.15	0.48	0.264
	C	0.432	0.404	0.32	1.466	0.212	0.268	0.34	1.07
	R^2	0.903	0.865	0.905	0.868	0.922	0.92	0.91	0.883

Table 4. Langmuir, Freundlich, Temkin and D-R isotherm parameters for the adsorption of BTEX by Bt-HDTMA and Bt-TMPA

Adsorbent	Adsorbate	Langmuir			Freundlich			Temkin			Dubnin Radushkevick		
		Qm(mg/g)	b(L/mg)	R^2	K_f(mg/g)	n	R^2	A(L/mg)	b	R^2	q_m(mg/g)	E(KJ/mol)	R^2
Bt-HDTMA	B	6.135	0.083	0.765	0.432	0.687	0.998	0.037	0.669	0.561	6.488	0.048	0.984
	T	5.882	0.0887	0.829	0.457	0.664	0.982	0.037	0.686	0.574	6.533	0.0485	0.954
	E	9.803	0.118	0.929	0.821	0.745	0.993	1.487	11.674	0.001	7.933	0.072	0.988
	X	16.949	0.138	0.772	2.689	0.753	0.979	443.34	0.265	0.664	15.41	0.0788	0.977
Bt-TMPA	B	10.753	0.0503	0.854	0.48	0.786	0.98	0.0179	0.612	0.864	6.166	0.0476	0.887
	T	6.097	0.196	0.998	1.649	0.552	0.991	10.75	0.351	0.323	6.296	0.104	0.97
	E	6.098	0.225	0.895	2.07	0.654	0.989	61.967	0.466	0.543	8.679	0.089	0.987
	X	23.81	0.253	0.979	5.038	1.554	0.996	0.088	-4.15	0.006	11.929	0.108	0.976

3.5 Intra-Particulate Diffusivity

The intraparticulate diffusivity was estimated using equation (7) which was developed using the linear driving force concept [75].

$$\ln(1-\alpha) = -Kpt \qquad (7)$$

Where α is the fractional attainment to equilibrium (FATE) given by equation (8), Kp is the rate constant for intraparticulate diffusivity

$$\alpha = \frac{[M]_t}{[M]} \qquad (8)$$

Where $[M]_t$ represents amount of BTEX adsorbed at time *t* and [M] the amount of BTEX adsorbed at infinity. The plot of the fractional attainment to equilibrium (FATE) is shown in figures 4a, and 4b for HDTMA modified bentonite (Bt-HDTMA) and TMPA modified bentonite (Bt-TMPA) respectively. FATE helps to ascertain in detail how equilibrium was approached by both the modified and unmodified clay adsorbents. All values of alpha coverage to 1 (one), showing that equilibrium was reached. The adsorption of benzene, toluene, ethylbenzene and xylene reached equilibrium in 120 mins for Bt-HDTMA and Bt-TMPA, implying higher sorption rate [76,77].

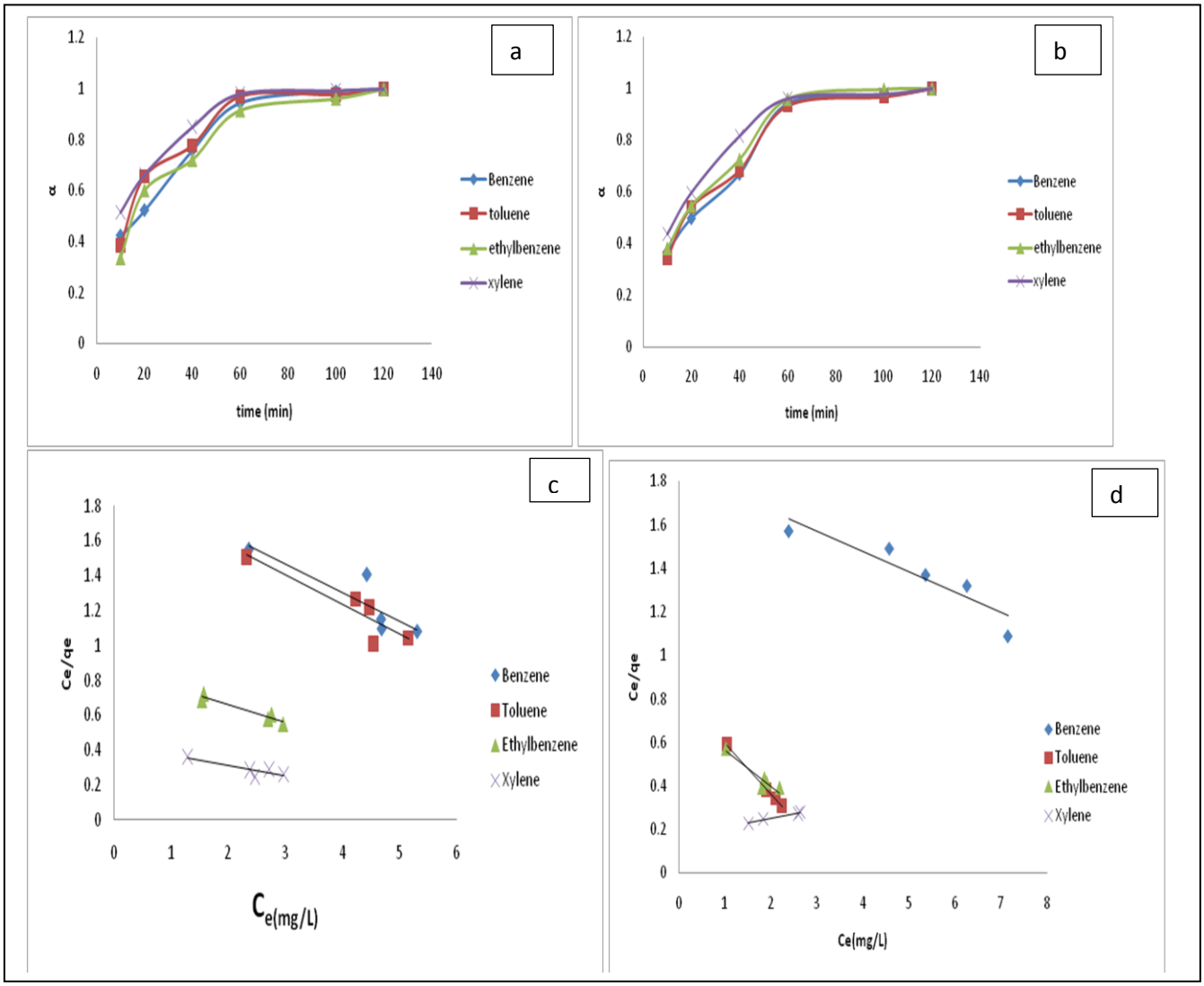

Figure 4: Fractional attainment to equilibrium (FATE), alpha against Time (min) for BTEX adsorption on Bt-HDTMA (a) and Bt-TMPA (b), (BTEX conc = 50mg/L); Isotherm models for: Bt-HDTMA-Langmiur (c), Bt-TMPA-Langmiur (d).

3.6 Adsorption Isotherm

Adsorption isotherm is one of the most crucial parameters used to find the adsorption mechanism necessary for designing any sorption system. It could be regarded as a graphical expression which described the amount or the quantity of the adsorbate that has been adsorbed onto the surface of the adsorbent at a particular operating condition. Adsorption isotherms are precisely used to ascertain whether the adsorbent could be efficiently exploited for the removal of the adsorbate molecule from several solutions [78]. The use of adsorption isotherm model helps one to understand the process of adsorption [79]. The two widely used adsorption isotherm models include; Langmuir and Freundlich adsorption isotherm models [8,79,80].

3.7 Langmuir Isotherm Model

This is a mathematical isotherm model, which is gotten from theoretical approach or non experimental analysis and also has a constant referred to as Langmuir constant. The Langmuir isotherm model assumes that the adsorption of adsorbate molecule can only occur at a homogeneous site of the adsorbent and when this happen, no other adsorption will take place on the adsorbent surface [8,78-80]. This isotherm model [83] in linear form is given as:

$$\frac{C_e}{q_e} = \frac{C_e}{Q_m} + \frac{1}{bQ_m} \qquad (9)$$

Where C (mg/L) and q_e (mg/g) are the concentration of adsorbate and the adsorption capacity of the adsorbent at the equilibrium time, respectively. b (L/mg) is the Langmuir constant and Q_m (mg/g) is maximum adsorbent capacity. Q_m and b are attained by the slope and intercept of C_e/q_e versus C_e, respectively. The values of the Langmuir isotherm parameters are shown in Table 4. Langmuir isotherm rather fitted poorly to the experimental data. Similar result was obtained by Nourmoradi *et al.* [8].

3.8 Freundlich Isotherm Model

The Freundlich isotherm model is an empirical adsorption isotherm model which explains the equilibrium relationships existing between the adsorbate and the adsorbent molecules and assumes multilayer adsorption on the adsorbent heterogeneous site. The Freundlich isotherm model [78,80,81] is given as:

$$ln\, q_e = ln\, k_f + \frac{1}{n}\, lnC_e \qquad (10)$$

q_e and C_e are the adsorption capacity (mg/g) and the concentration (mg/L) of the adsorbate at equilibrium. The values of 1/n and k_f are gotten from the linear plot of In q_e against In C_e. 1/n is the slope of the graph while k_f is the intercept on y-axis, which are the Freundlich constant relating to heterogeneity of

the adsorbent surface and adsorption capacity respectively [80]. The Freundlich isotherm parameters and its correlation coefficient (R^2) for BTEX adsorption by Bt-HDTMA and Bt-TMPA are exhibited in Table 4; Figures 5e and 5f. From the results, Freundlich isotherm model fitted well to the experimental data. Many researchers have reported that sorption of BTEX from aqueous solutions with different adsorbents is well described by Freundlich isotherm model [8,41,43,44,46]. The n values ranging from 0.55-1.55 obtained by this isotherm model showed that BTEX is suitably adsorbed by Bt-HDTMA and Bt-TMPA, indicating strong adsorption bonds between organoclays and BTEX compounds. Nourmoradi *et al*., [8] and Sharmasarkar *et al*., [46] reported that the n values for the removal of BTEX via the cationic modified clays (TTAB-Mt) and (TMPA-SWy and Adam-SWy) were in the range of 1.04 to 1.55 and 1.59 to 1.88 respectively.

3.9 Dubnin-Radushkevich Isotherm Model

The Dubinin-Radushkevich isotherm (D-R) model has been used to ascertain the type of sorption process as physical, chemical adsorption or ion exchange [8,81]. The linear form of the D-R isotherm model can be represented as:

$$ln\ q_e = ln\ q_m - \beta\varepsilon^2 \qquad (11)$$

where, q_m (mg/g) is the theoretical sorption capacity based on the isotherm, β (kJ/mol) is related to mean adsorption energy and ε (Polanyi Potential) is equal to RT ln (1 + 1/Ce). R (kJ/mol^{-} K) is the universal gas constant and (K) is temperature [81]. From Figures 5c and 5d, q_m and β are obtained from the intercept and slope lnq_e versus ε^2, respectively. β (kJ/mol) is the mean adsorption energy that is represented by equation (12):

$$E = \frac{1}{\sqrt{2\beta}} \qquad (12)$$

The type of adsorption process is specified by the E value as follow: Physisorption or Chemisorption occurs if E < 8 kJ/mol or E > 16 kJ/mol, respectively. But the chemical ion exchange occurs for E in the 8-16 kJ/mol [82]. The values of parameters for D-R isotherm model for adsorption of BTEX by Bt-HDTMA and Bt-TMPA are displayed in Table 4. As seen, the adsorption of BTEX by Bt-HDTMA and Bt-TMPA has occurred for E values in the range of 0.048-0.079 and 0.048-0.11 kJ/mol for Bt-HDTMA and Bt-TMPA respectively. Hence, the removal of BTEX in the solution by Bt-HDTMA and Bt-TMPA is governed by physisorption.

3.10 Temkin Isotherm Model

The Temkin model accounts for the effects of indirect adsorbate-adsorbate interactions on the adsorption isotherm, with heat of adsorption tending to decrease with increasing coverage due to these interactions [39,70]. Temkin model assumes a linear decrease in the heat of adsorption with temperature, rather than logarithmic decrease as implied by the Freundlich equation. The linear form of the Temkin model is given by Eq. (13).

$$q_e = \frac{RT}{b} lnA + \frac{RT}{b} lnC_e \qquad (13)$$

where A ($L.mg^{-1}$) and b are Temkin isotherm constants, R = $0.0083kJmol^{-1}$ K^{-1} and T is temperature (K) of the experiment. A plot of q_e versus InC_e is linear and the Temkin constants determined from the slope and intercept. From figures 5e and 5f, it can be seen that the Temkin isotherm fitted rather poorly to the experimental data. Similar result was also obtained by Egbuchunam *et al.,* [70].

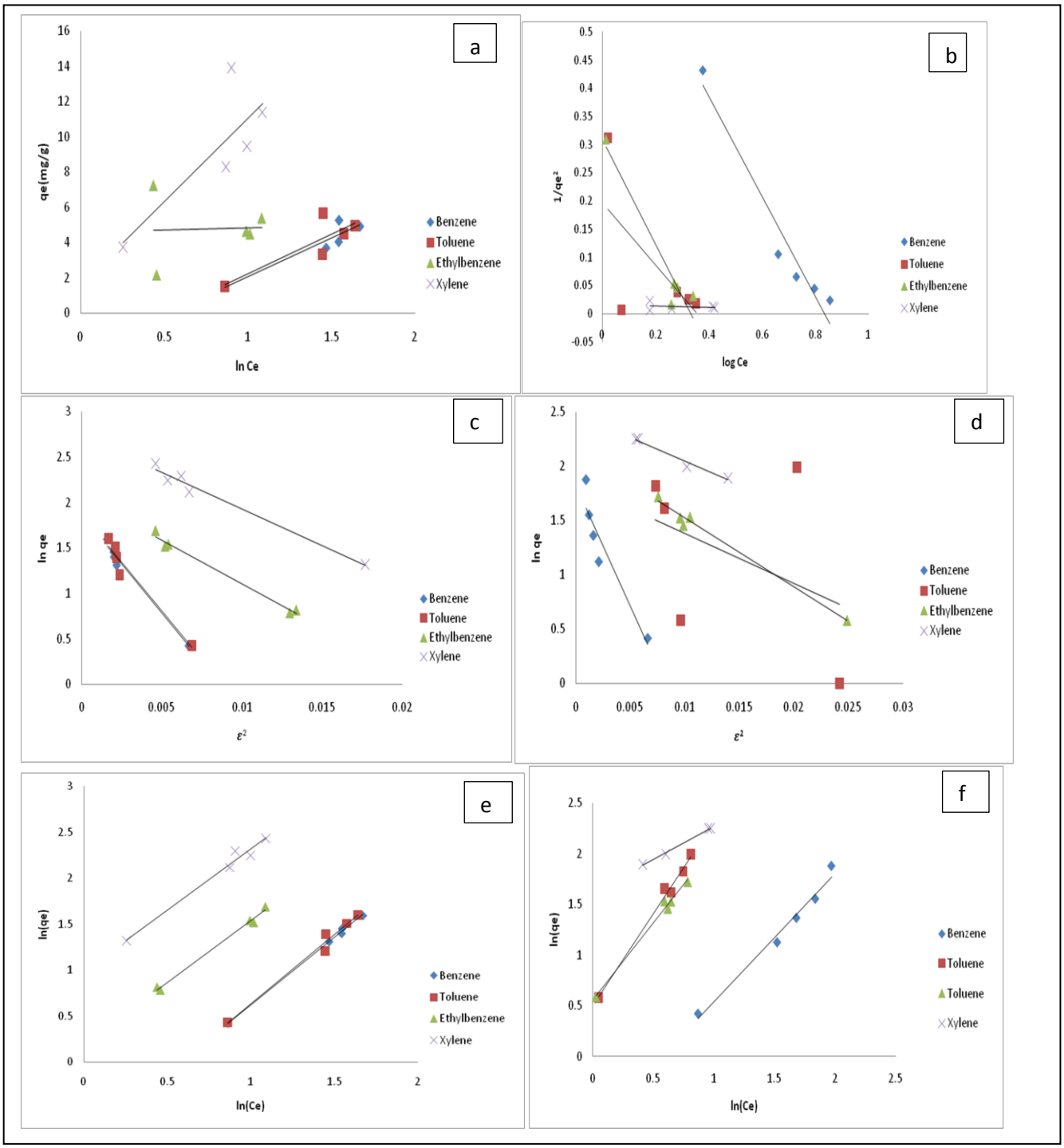

Figure 5: Isotherm models for the adsorption of BTEX by: Bt-HDTMA-Temkin (a), Bt-TMPA-Temkin (b), Bt-HDTMA-D-R (c), Bt-TMPA-D-R (d), Bt-HDTMA-Freundlich (e), Bt-TMPA-Freundlich (f).

4. Conclusion

In this study, the effectiveness of hexadecyltrimethylammonium (HDTMA) and Trimethylphenylammonium (TMPA) cations intercalation with Bentonite clay, corresponding to 100% of the cation exchange capacity (CEC) in the removal of benzene, toluene, ethylbenzene and xylene (BTEX) in aqueous solution was investigated with contact time of 2 hours. BTEX adsorption onto Bt-HDTMA and Bt-TMPA was well described by the pseudo-second-order kinetic and Freundlich isotherm models. The result of the present study indicates that bentonite modified with HDTMA and TMPA can be successfully employed for the removal of BTEX over a concentration range and at varying contact time. In addition, the modified bentonite has the potential to replace the high cost adsorbents such as diatomite, activated carbon, zeolites, etc, owing to its high surface area, low cost, eco-friendly , non-toxic and great adsorption capacity.

Acknowledgement

This research did not receive any specific grant from funding agencies.

Conflict of Interest

Authors declare no conflict of interest.

References

1. Ehanathan S, Raagulan K, Rajapakse RG, et al. Groundwater quality in the Jaffna peninsula of Sri Lanka and a qualitative study of BTEX removal by greenly synthesized iron nanoparticles-electro-catalyst system. Groundwater for Sustainable Development (2020): 100362.
2. Marara T, Palamuleni LG. An environmental risk assessment of the Klip river using water quality indices. Physics and Chemistry of the Earth, Parts A/B/C 114 (2019): 102799.
3. Owa FD. Water pollution: sources, effects, control and management. Mediterranean Journal of Social Sciences 4 (2013): 65.
4. US EPA (United States Environmental Protection Agency), 2008. MARPOL 73/78. http://www.epa.gov/owow/OCPD/marpol.html (2008).
5. Egwaikhide PA, Akporhonor EE, Okieimen FE. Utilization of coconut fibre carbon in the removal of soluble petroleum fraction polluted water. International Journal of Physical Sciences 2 (2007): 47-49.
6. Fedorov K, Plata-Gryl M, Khan JA, et al. Ultrasound-assisted heterogeneous activation of persulfate and peroxymonosulfate by asphaltenes for the degradation of btex in water. Journal of Hazardous Materials (2020): 122804.
7. EUR-Lex, EUR-Lex - 32004L0042 - EN, 2004.
8. Nourmoradi H, Khiadani M, Nikaeen M. Multi-component adsorption of benzene, toluene, ethylbenzene, and xylene from aqueous solutions by montmorillonite modified with tetradecyl trimethyl ammonium bromide. Journal of Chemistry (2013).

9. Smith MR. The biodegradation of aromatic hydrocarbons by bacteria. Biodegradation 1 (1990): 191-206.
10. Latif MT, Abd Hamid HH, Ahamad F, et al. BTEX compositions and its potential health impacts in Malaysia. Chemosphere 237 (2019): 124451.
11. Mirrezaei MA, Orkomi AA. Gas flares contribution in total health risk assessment of BTEX in Asalouyeh, Iran. Process Safety and Environmental Protection (2020).
12. Lara-Ibeas I, Megias-Sayago C, Rodríguez-Cuevas A, et al. Adsorbent screening for airborne BTEX analysis and removal. Journal of Environmental Chemical Engineering 8 (2020): 103563.
13. Mohammadi A, Ghassoun Y, Löwner MO, et al. Spatial analysis and risk assessment of urban BTEX compounds in Urmia, Iran. Chemosphere 246 (2020): 125769.
14. Mello JM, Brandão HL, Valério A, et al. Biodegradation of BTEX compounds from petrochemical wastewater: Kinetic and toxicity. Journal of Water Process Engineering 32 (2019): 100914.
15. Megías-Sayago C, Lara-Ibeas I, Wang Q, et al. Volatile organic compounds (VOCs) removal capacity of ZSM-5 zeolite adsorbents for near real-time BTEX detection. Journal of Environmental Chemical Engineering 8 (2020): 103724.
16. Vaezihir A, Bayanlou MB, Ahmadnezhad Z, et al. Remediation of BTEX plume in a continuous flow model using zeolite-PRB. Journal of Contaminant Hydrology 230 (2020): 103604.
17. Akinsanya B, Ayanda IO, Onwuka B, et al. Bioaccumulation of BTEX and PAHs in Heterotis niloticus (Actinopterygii) from the Epe Lagoon, Lagos, Nigeria. Heliyon 6 (2020): e03272.
18. Zhao L, Qin X, Hou X, et al. Research on determination of BTEX in human whole blood using purge and trap-gas chromatography-mass spectrometry combined with isotope internal standard. Microchemical Journal 145 (2019): 308-312.
19. Pawlowski MH. Analytical and Field Test Methods for Measuring BTEX Metabolite Occurrence and Transport in Groundwater. Oregon State Univ Corvallis Dept Of Chemistry (1998).
20. Boczkaj G, Fernandes A. Wastewater treatment by means of advanced oxidation processes at basic pH conditions: a review. Chemical Engineering Journal 320 (2017): 608-633.
21. Miri M, Shendi MR, Ghaffari HR, et al. Investigation of outdoor BTEX: Concentration, variations, sources, spatial distribution, and risk assessment. Chemosphere 163 (2016): 601-609.
22. Grady SJ, Casey GD. Occurrence and distribution of methyl tert-butyl ether and other volatile organic compounds in drinking water in the Northeast and Mid-Atlantic regions of the United States, 1993-

98. US Department of the Interior, US Geological Survey (2001).
23. Schmidt TC, Haderlein SB, Pfister R, et al. Occurrence and fate modeling of MTBE and BTEX compounds in a Swiss Lake used as drinking water supply. Water Research 38 (2004): 1520-1529.
24. Mitra S, Roy P. BTEX: A serious ground-water contaminant. Research Journal of Environmental Sciences 5 (2011): 394.
25. Reddy CM, Arey JS, Seewald JS, et al. Composition and fate of gas and oil released to the water column during the Deepwater Horizon oil spill. Proceedings of the National Academy of Sciences 109 (2012): 20229-20234.
26. Bolden AL, Kwiatkowski CF, Colborn T. New look at BTEX: are ambient levels a problem?. Environmental Science & Technology 49 (2015): 5261-5276.
27. El-Hashemy MA, Ali HM. Characterization of BTEX group of VOCs and inhalation risks in indoor microenvironments at small enterprises. Science of The Total Environment 645 (2018): 974-983.
28. Pouresmaeili MA, Aghayan I, Taghizadeh SA. Development of Mashhad driving cycle for passenger car to model vehicle exhaust emissions calibrated using on-board measurements. Sustainable Cities and Society 36 (2018): 12-20.
29. Ran J, Qiu H, Sun S, Tian L. Short-term effects of ambient benzene and TEX (toluene, ethylbenzene, and xylene combined) on cardiorespiratory mortality in Hong Kong. Environment international. 2018 Aug 1;117: 91-98.
30. Wilbur S, Bosch S. Interaction profile for: benzene, toluene, ethylbenzene, and xylenes (BTEX). Agency for Toxic Substances & Disease Registry (ATSDR) (2004).
31. Abbasi F, Pasalari H, Delgado-Saborit JM, et al. Characterization and risk assessment of BTEX in ambient air of a Middle Eastern City. Process Safety and Environmental Protection 139 (2020): 98-105.
32. Chen D, Zhang ZJ, Gao FL. Study on health risk assessment of aromatic hydrocarbons from a typical oil refinery in Pearl River Delta. China 37 (2017): 1961-1970.
33. Dehghani M, Fazlzadeh M, Sorooshian A, et al. Characteristics and health effects of BTEX in a hot spot for urban pollution. Ecotoxicology and Environmental Safety 155 (2018): 133-143.
34. Hu R, Liu G, Zhang H, et al. Levels, characteristics and health risk assessment of VOCs in different functional zones of Hefei. Ecotoxicology and Environmental Safety 160 (2018): 301-307.
35. Hajizadeh Y, Mokhtari M, Faraji M, et al. Trends of BTEX in the central urban area of Iran: A preliminary study of photochemical ozone pollution and health risk assessment. Atmospheric Pollution Research 9 (2018): 220-229.
36. Zheng H, Kong S, Xing X, et al. Monitoring of volatile organic compounds (VOCs) from an oil and gas station in northwest China for

1 year. Atmospheric Chemistry & Physics 18 (2018).

37. Kitwattanavong M, Prueksasit T, Morknoy D, et al. Health risk assessment of petrol station workers in the inner city of Bangkok, Thailand, to the exposure to BTEX and carbonyl compounds by inhalation. Human and Ecological Risk Assessment: An International Journal 19 (2013): 1424-1439.
38. Phatrabuddha N, Maharatchpong N, Keadtongtawee S, et al. Comparison of Personal BTEX Exposure and Pregnancy Outcomes among Pregnant Women Residing in and Near Petrochemical Industrial Area. EnvironmentAsia 6 (2013).
39. Vidal CB, Raulino GS, Barros AL, et al. BTEX removal from aqueous solutions by HDTMA-modified Y zeolite. Journal of Environmental Management 112 (2012): 178-185.
40. Aivalioti M, Pothoulaki D, Papoulias P, et al. Removal of BTEX, MTBE and TAME from aqueous solutions by adsorption onto raw and thermally treated lignite. Journal of Hazardous Materials 207 (2012): 136-146.
41. Lin SH, Huang CY. Adsorption of BTEX from aqueous solution by macroreticular resins. Journal of Hazardous Materials 70 (1999): 21-37.
42. Daifullah AA, Girgis BS. Impact of surface characteristics of activated carbon on adsorption of BTEX. Colloids and Surfaces A: Physicochemical and Engineering Aspects 214 (2003): 181-193.
43. Su F, Lu C, Hu S. Adsorption of benzene, toluene, ethylbenzene and p-xylene by NaOCl-oxidized carbon nanotubes. Colloids and Surfaces A: Physicochemical and Engineering Aspects 353 (2010): 83-91.
44. Aivalioti M, Vamvasakis I, Gidarakos E. BTEX and MTBE adsorption onto raw and thermally modified diatomite. Journal of Hazardous Materials 178 (2010): 136-143.
45. Vianna MM, Valenzuela-Díaz FR, Kozievitch VF, et al. Synthesis and characterization of modified clays as sorbents of toluene and xylene. InMaterials Science Forum 498 (2005): pp. 691-696.
46. Sharmasarkar S, Jaynes WF, Vance GF. BTEX sorption by montmorillonite organo-clays: TMPA, ADAM, HDTMA. Water, Air, and Soil Pollution. 2000 Apr 1;119(1-4):257-73.
47. Park Y, Ayoko GA, Horváth E, et al. Structural characterisation and environmental application of organoclays for the removal of phenolic compounds. Journal of Colloid and Interface Science 393 (2013): 319-334.
48. Hu B, Luo H. Adsorption of hexavalent chromium onto montmorillonite modified with hydroxyaluminum and cetyltrimethylammonium bromide. Applied Surface Science 257 (2010): 769-775.
49. Zhou Y, Jin XY, Lin H, Chen ZL. Synthesis, characterization and potential application of organobentonite in removing 2, 4-DCP from industrial wastewater. Chemical Engineering Journal 166 (2011): 176-183.

50. De Paiva LB, Morales AR, Díaz FR. Organoclays: properties, preparation and applications. Applied Clay Science 42 (2008): 8-24.
51. Jaynes WF, Vance GF. Sorption of benzene, toluene, ethylbenzene, and xylene (BTEX) compounds by hectorite clays exchanged with aromatic organic cations. Clays and Clay Minerals 47 (1999): 358-365.
52. Sharafimasooleh M, Bazgir S, Tamizifar M, et al. Adsorption of hydrocarbons on modified nanoclays. InIOP Conference Series Materials Science and Engineering 18 (2011): p. 182012).
53. Baskaralingam P, Pulikesi M, Ramamurthi V, et al. Equilibrium studies for the adsorption of acid dye onto modified hectorite. Journal of Hazardous Materials136 (2006): 989-992.
54. Banik N, Jahan SA, Mostofa S, et al. Synthesis and characterization of organoclay modified with cetylpyridinium chloride. Bangladesh Journal of Scientific and Industrial Research 50 (2015): 65-70.
55. Trivedi HC, Patel VM, Patel RD. Adsorption of cellulose triacetate on calcium silicate. European Polymer Journal 9 (1973): 525-531.
56. Kittrick JA. Cholesterol as a Sta Kittrick JA. Cholesterol as a Standard in the X-Ray Diffraction of Clay Minerals. Soil Science Society of America Journal 24 (1960): 17-20.
57. Taleb K, Pillin I, Grohens Y, et al. Gemini surfactant modified clays: Effect of surfactant loading and spacer length. Applied Clay Science 161 (2018): 48-56..
58. Tiwari M, Bajpai VK, Sahasrabuddhe AA, et al. Inhibition of N-(4-hydroxyphenyl) retinamide-induced autophagy at a lower dose enhances cell death in malignant glioma cells. Carcinogenesis 29 (2008): 600-609.
59. Makochekanwa C, Bankovic A, Tattersall W, et al. Total and positronium formation cross sections for positron scattering from H2O and HCOOH. New Journal of Physics 11 (2009): 103036.
60. Khenifi A, Bouber Khenifi A, Bouberka Z, Sekrane F, Kameche M, Derriche Z. Adsorption study of an industrial dye by an organic clay. Adsorption 13 (2007): 149-158.
61. Carvalho MN, Da Motta M, Benachour M, et al. Evaluation of BTEX and phenol removal from aqueous solution by multi-solute adsorption onto smectite organoclay. Journal of Hazardous Materials 239 (2012): 95-101.
62. Ikhtiyarova GA, Özcan AS, Gök Ö, et al. Characterization of natural-and organobentonite by XRD, SEM, FT-IR and thermal analysis techniques and its adsorption behaviour in aqueous solutions. Clay Minerals 47 (2012): 31-44.
63. Obi C, Okike UN, Okoye PI. The Use of Organophilic Bentonite in the Removal Phenol from Aqueous Solution: Effect of Preparation Techniques. Modern Chem Appl 6 (2018).

64. Özcan AS, Erdem B, Özcan A. Adsorption of Acid Blue 193 from aqueous solutions onto Na–bentonite and DTMA–bentonite. Journal of Colloid and Interface Science 280 (2004): 44-54.
65. Dan CH, Lee MH, Kim YD, et al. Effect of clay modifiers on the morphology and physical properties of thermoplastic polyurethane/clay nanocomposites. Polymer 47 (2006): 6718-6730.
66. Olugbenga AG, Garba MU, Soboyejo W, et al. Beneficiation and characterization of a bentonite from Niger Delta Region of Nigeria. International Journal of Science and Engineering Investigations 2 (2013): 14-18.
67. Gitipour S, Bowers MT, Bodocsi A. The use of modified bentonite for removal of aromatic organics from contaminated soil. Journal of Colloid and Interface Science 196 (1997): 191-198.
68. Ma YH, He HP, Zhu JX. Influence of Cation Exchange Capacity and Numbers of Alkyl-Chains on the Property of Organo-Montmorillonites. Acta Mineralogica Sinica 9 (2010): 11-30..
69. Bandura L, Kołodyńska D, Franus W. Adsorption of BTX from aqueous solutions by Na-P1 zeolite obtained from fly ash. Process Safety and Environmental Protection 109 (2017): 214-223.
70. Egbuchunam TO, Obi C, Okieimen FE, et al. Removal of BTEX from aqueous solution using organokaolinite. International Journal of Applied Environmental Sciences 11 (2016): 505-513.
71. Makhathini TP, Rathilal S. Investigation of BTEX compounds adsorption onto polystyrenic resin. South African Journal of Chemical Engineering 23 (2017): 71-80.
72. Lian Q, Konggidinata MI, Ahmad ZU, et al. Combined effects of textural and surface properties of modified ordered mesoporous carbon (OMC) on BTEX adsorption. Journal of Hazardous Materials 377 (2019): 381-390.
73. Ho YS, McKay G. Sorption of dye from aqueous solution by peat. Chemical Engineering Journal 70 (1998): 115-124.
74. Jiang MQ, Jin XY, Lu XQ, et al. Adsorption of Pb (II), Cd (II), Ni (II) and Cu (II) onto natural kaolinite clay. Desalination 252 (2010): 33-39.
75. Okieimen FE, Okundia EU, Ogbeifun DE. Sorption of cadmium and lead ions on modified groundnut (Arachis hypogea) husks. Journal of Chemical Technology & Biotechnology 51 (1991): 97-103.
76. Igwe JC, Mbonu OF, Abia AA. Sorption kinetics, intraparticle diffusion and equilibrium partitioning of azo dyes on great millet (Andropogon sorghum) waste biomass. JApSc 7 (2007): 2840-2847.
77. Okpareke OC, Agha II, Ejikeme PM. Removal of Cu (II), Cd (II) and Hg (II) ions from simulated waste water by Brachystagea Eurycoma seed pod: Intraparticle diffusivity and sorption studies. In32nd. International Conference of the Chemical Society of Nigeria, Bauchi (2009).

78. Emam EA. Modified activated carbon and bentonite used to adsorb petroleum hydrocarbons emulsified in aqueous solution. Am J Environ Prot 2 (2013): 161-169.
79. Senturk HB, Ozdes D, Gundogdu A, et al. Removal of phenol from aqueous solutions by adsorption onto organomodified Tirebolu bentonite: Equilibrium, kinetic and thermodynamic study. Journal of Hazardous Materials 172 (2009): 353-362.
80. Ewuzie Henry E, Ekpo Rose E, Okeacha Ezinne G. Multi Component Adsorption of Toluene, Ethyl Benzene and Meta-Xylene by Batch Adsorption Technique Using Natural and Acid Treated-Modified Sodium Bentonite..
81. Koyuncu H, Yıldız N, Salgın U, et al. Adsorption of o-, m-and p-nitrophenols onto organically modified bentonites. Journal of Hazardous Materials 185 (2011): 1332-1339.
82. Cestari AR, Vieira EF, Vieira GS, et al. Aggregation and adsorption of reactive dyes in the presence of an anionic surfactant on mesoporous aminopropyl silica. Journal of Colloid and Interface Science 309 (2007): 402-411.
83. Li Y, Ma S, Xu S, et al. Novel magnetic biochar as an activator for peroxymonosulfate to degrade bisphenol A: Emphasizing the synergistic effect between graphitized structure and CoFe2O4. Chemical Engineering Journal 387 (2020): 124094.